OPEN ACCESS

University of Dundee

University of Dundee

Depth Evaluation of Soft Tissue Mimicking Phantoms Using Surface Acoustic Waves

Li, C.; Li, S.; Wei, C.; Wang, R. K.; Huang, Z.

Published in:
Physics Procedia

DOI:
10.1016/j.phpro.2015.03.029

Publication date:
2015

Licence:
CC BY-NC-ND

Document Version
Publisher's PDF, also known as Version of record

Link to publication in Discovery Research Portal

Citation for published version (APA):
Li, C., Li, S., Wei, C., Wang, R. K., & Huang, Z. (2015). Depth Evaluation of Soft Tissue Mimicking Phantoms Using Surface Acoustic Waves. *Physics Procedia*, *63*, 177-181. https://doi.org/10.1016/j.phpro.2015.03.029

General rights
Copyright and moral rights for the publications made accessible in Discovery Research Portal are retained by the authors and/or other copyright owners and it is a condition of accessing publications that users recognise and abide by the legal requirements associated with these rights.

• Users may download and print one copy of any publication from Discovery Research Portal for the purpose of private study or research.
• You may not further distribute the material or use it for any profit-making activity or commercial gain.
• You may freely distribute the URL identifying the publication in the public portal.

Take down policy
If you believe that this document breaches copyright please contact us providing details, and we will remove access to the work immediately and investigate your claim.

Download date: 10. Aug. 2022

Available online at www.sciencedirect.com

ScienceDirect

Physics Procedia 63 (2015) 177 – 181

Physics Procedia

43rd Annual Symposium of the Ultrasonic Industry Association, UIA Symposium 2014

Depth evaluation of soft tissue mimicking phantoms using surface acoustic waves

C. Li[a,b], S. Li[a], C. Wei[a], R. K. Wang[b] and Z. Huang[a,]

[a]*School of Engineering, Physics and Mathematics, University of Dundee, Dundee, UK*
[b]*Department of Bioengineering, University of Washington, Seattle, USA*

Abstract

Surface acoustic wave (SAW) shows advantages in revealing skin mechanical properties. In this paper, we evaluates the elasticity of tissue mimicking phantoms by inversion of SAWs phase velocity to Young's Modulus, the estimated SAWs evaluating depth is determined based on the assumption of that SAWs penetration approximately equals one wavelength. The tissue mimicking phantoms are made of agar with concentration of 1%, 2% and 3%. Their elasticity tested from our system is 13.3kPa, 53.4kPa and 257.9kPa respectively, with expected gradient. The evaluation depth is then estimated as 0.542mm to 3.403mm underneath the phantom surface, which indicates that this method is suitable to measure elasticity in dermis layer of skin.

© 2015 Published by Elsevier B.V. This is an open access article under the CC BY-NC-ND license
(http://creativecommons.org/licenses/by-nc-nd/4.0/).
Peer-review under responsibility of the Ultrasonic Industry Association

Keywords: component; Surface acoustic waves (SAWs); phase velocity; elasticity properties, tissue;

1. Introduction

Mechanical properties of skin such as the elasticity are useful for understanding skin patho-physiology, which can aid medical diagnosis and treatment. There are several ways to characterize soft tissue elasticity, such as using ultrasound elastography (Rivaz et al., 2011, Uff et al., 2009, Zhu et al., 2008), acoustic radiation force impulse elastography (ARFIE) (Palmeri et al., 2011, Nightingale et al., 2003) and magnetic resonance elastography (MRE) (Wang et al., 2011, Mariappan et al., 2011) etc. Nevertheless, most of them are tracking in-vivo shear wave propagation, thus low imaging resolutions are normally given by these systems around the tissue surface region. In addition, many of them are not truly quantitative, presenting further limitations in quantifying the elastic property of skin. In comparison, surface acoustic waves have many advantages in skin characterization, as the dominant energy of SAWs is located at the surface. For broadband SAWs, different frequency contents penetrate different depth. Therefore low frequency content of SAWs propagates at a velocity determined by skin subtractive layer, and high frequency content of SAWs propagates with the velocity determined by skin surface layer.

1875-3892 © 2015 Published by Elsevier B.V. This is an open access article under the CC BY-NC-ND license
(http://creativecommons.org/licenses/by-nc-nd/4.0/).
Peer-review under responsibility of the Ultrasonic Industry Association
doi:10.1016/j.phpro.2015.03.029

In our previous study (Li et al., 2011a), SAWs are generated by short laser pulses which are broadly referred as laser ultrasound. Laser generated SAWs is based on the thermal elastic regime in which the electro-magnetic energy of photons is firstly converted to a localized heating in tissue and then converted again to the acoustic waves due to the aroused thermal expansion (Li et al., 2011b, Chunhui et al., 2010). Alternatively, SAWs can be stimulated by a pulsed vibration. In this paper, we employed an electro-magnetic shaker to deliver the dynamic vibration on phantoms to generate SAWs and using a 633nm laser probe that are perpendicular incident on the phantoms to detect the generated surface acoustic waves based on the effect of optical Doppler shift. Comparing with laser ultrasound, shaker generation of SAWs is much more cost-effective and safe when it takes into the real clinical circumstance.

2. Theory

The elasticity of tissue mimicking phantoms will be estimated by phase velocity of SAWs and then inversing the Young's Modulus.

2.1. Phase velocity

Phase velocity of a wave is defined as the speed at which the phase of any one frequency component of a wave propagates. A more straight explanation is that the phase velocity can be regarded as a spectral analysis of wave propagation speed. In homogeneous materials, the phase velocity of SAWs would be identical at each frequency; meantime the value of phase velocity actually equals the group velocity of a wave. However, dispersion of SAWs phase velocity will be observed when the material become with layered characteristics, that is to say, different band waves will propagate at different wave speeds. The phase velocity of a wave can be calculated by the measurement of phase change with respect to the wave journey distance as follows:

$$C_r = 2\pi f \left| \Delta r / \Delta \varphi \right| \tag{1}$$

where C_r is the component of SAWs phase velocity at a certain frequency f and $\Delta\varphi$ is the variation of wave phase when the wave has moved a distance Δr.

2.2. Phase velocity and elasticity

The phase velocity can be related to the elasticity of materials as follows,

$$C_s = \frac{0.87 + 1.12\upsilon}{1+\upsilon} \sqrt{\frac{E}{2\rho(1+\upsilon)}} \tag{2}$$

where p is the density of material, υ is the passion's ratio and E is the Young's Modulus. For soft materials like tissue, the equation can come down to a simpler form without taking the consideration of passion's ratio as:

$$C_s = \frac{1}{1.05} \sqrt{\frac{E}{3\rho}} \tag{3}$$

Therefore, the Young's Modulus can be easily inverted from the phase velocity as long as we know the density of tissue.

3. Experiment setup

The experiment set-up is showed in the figure 1. In the system, SAWs are generated by an electro-magnetic shaker which provides a short pulse oscillation on the surface of phantoms to stimulate SAWs. A bar shape design is attached on the shaker as a line wave stimulus source. The shaker is driven by 20Hz square wave sequences from the functional generator with a duty cycle of 50%. The voltage of driven signal is set to be 3V (peak to peak value) and the offset of that is -1.5V.

The shaker was mounted on a robotic arm to provide precise position in both lateral (x) and vertical (y) directions as shown in figure 1. As stated in section II, distance and phase difference between two detection points on the wave path are the essential terms to calculate the phase velocity. In the experiment, the shaker lateral mobile steps are set as 1mm, giving uniform distribution of distance between wave source and detection point. The shaker vertical mobile steps are kept as 0.01mm, a much smaller interval than lateral one, as the extent of contact between the shaker and phantoms are very subtle for the generation of robust SAWs. The robotic arm commutates with PC via port RS-232 in a customized Labview program, receiving movement commands and feeding back current position coordinates.

SAWs are detected by Laser-vibrometer and displayed on the oscilloscope, also recorded on Labview program. The vibrometer sensor head emits objective laser probes direct incident on the surface and collects the reflected signal together with a reference beam into the embedded CCD camera. Optical interference can be obtained when the two coherent light beams are made coincide. Vibration on surface arise phase difference and results in a vibrational optical intensity on the CCD. By counting the interference fringe pattern moving on the detector, the out of plane displacement versus time information of the surface vibration can be decoded. The distance between laser sensor head and phantom are fixed at stand-off distance (295mm) to ensure the visibility maxima of optical detector.

Agar phantoms are used in the experiments to mimicking acoustic and mechanical behavior of human soft tissue. Phantoms are made as homogenous to eliminate any dispersion in phase velocity, which is essential for assessment and calibration process. Three phantoms have been made with 3% agar concentration, 2% agar concentration and 1% agar concentration respectively, from hard to soft. The phantom surfaces are flat and smooth, also painted with dark ink to enhance the surface optical reflection to increase the signal to noise ratio of the laser vibrometer. Procedures of making such phantoms are described as follows:

1. Take 110ml distilled water and heat it above 90 °C. (Considering evaporation, the distilled water should be more than ideal value - 100ml).
2. Stir the boiled water and pour into already weighted agar (1g for 1% agar phantom, 2g for 2% agar phantom and 3g for 3% agar phantom).
3. Keep stirring and heating the water until all agar resolves when liquid looks transparent without any impurity.
4. Stop heating when liquid remain exactly 100 ml. Wait for the liquid cooling down to 40 ~ 50 °C.
5. Pour dark inks and stir with a relative low speed (avoid bubbles).Keep stirring for around 5 minutes.
6. Wait for the liquid cooling to 30 ~ 40 °C, then pour into container for modeling.

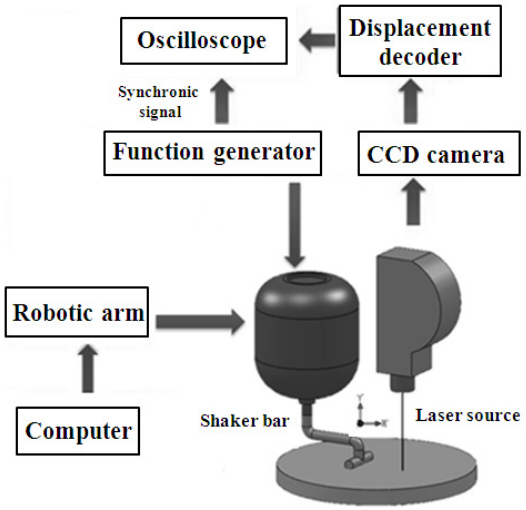

Figure1 Schematic diagram of experimental set-up for the generation and detection of SAWs on the surface of phantom

4. Results

SAWs signals are recorded at 6 points along wave propagation path on each agar phantoms. Figure 2 shows typical results of waveforms of SAWs on agar phantoms. The top wave in figure 2 is detected at 15 mm away the wave source and it keeps moving away with a uniform distance of 1mm for the rest waves. From the figure we can see the dominant wave energy locates at low frequencies and the body SAWs could sustain about 4ms.

The phase velocities of SAWs on 1% - 3% agar phantoms are calculated using equation 1 which it can be seen in figure 4. All of the phase velocities have no obvious dispersion, which is expected in homogeneous phantoms. However some small disturbances can be observed at the low frequency on 2% and 3% agar phantoms due to the system measurement error. In comparison, the system has a better performance on the 1% agar phantom where the phase velocity almost stays at the same value at each frequency. This may indicate that SAWs would be more effectively generated on soft specimen, and it is what we expected as the mechanical property of 1% agar phantom is very close to that of real tissue.

If we average the phase velocity cross the whole frequency spectrum, the phase velocity are estimated as 2.05m/s on 1% agar phantom, 3.96m/s on 2% agar phantom, and 6.13m/s on 3% agar phantom. Result show that SAWs propagate at a higher speed on hard specimen and on the contrary SAWs spread at lower speed on soft materials. Therefore the elasticity of materials can be unveiled from the phase velocity of surface acoustic waves. In order to get a quantification of the elasticity, the phase velocity on each phantoms are then inversed to the Young's modulus using equation 3. The density of three agar phantoms are all approximated into 1000 kg/m3, and the Young's modulus of them are then calculated as 13.2 kPa on 1% agar phantom, 53.4 kPa on 2% agar phantom and 257.9 kPa on 3% agar phantom. As reported in (Delalleau et al., 2006, Pailler-Mattei et al., 2008), Young's modulus of skin range from 5.67 kPa to 33kPa, therefore the 1% agar phantom has the most similar mechanical properties with skin.

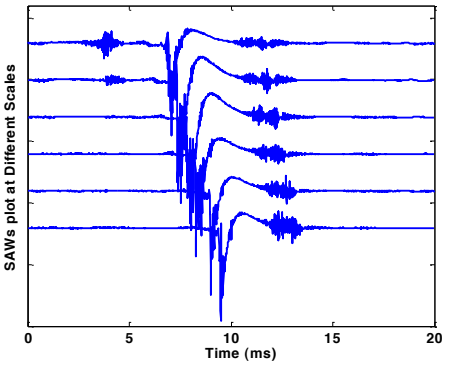

Fig.2 Typical SAWs waveforms detected at 15mm (top) and 20mm (bottom) away wave source

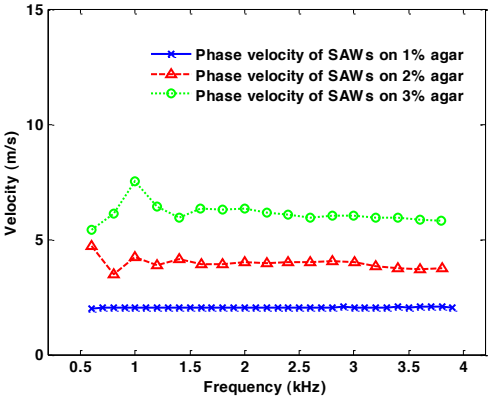

Fig.3 Phase velocity of SAWs on agar phantoms with different stiffness; SAWs propagate faster on hard phantoms while the velocity become slower on soft phantoms

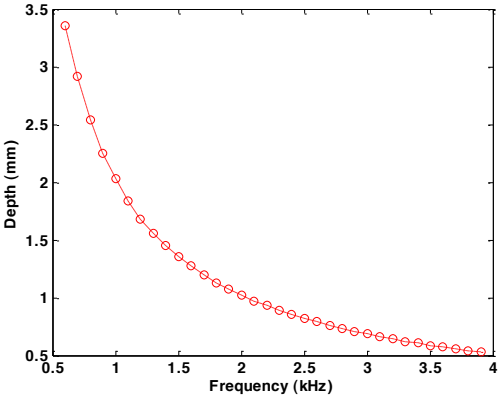

Fig.4 SAWs evaluating depth in 1% agar phantom; different frequency contents evaluate different depth

5. Conclusions

SAWs are generated by dynamic vibration that is delivered by an electro-magnetic shaker and received by a Doppler shift laser vibrometer in this paper. The SAWs are used to characterise three agar phantoms with concentration of 1%, 2% and 3% respectively, and the Young's modulus of them are estimated as 13.2 kPa, 53.4 kPa and 257.9 kPa. The results show that our system is capable to identify and quantify the elasticity of soft tissue mimicking phantoms with different stiffness. The characterisation depth of the SAWs on 1% agar phantom is then estimated based on the assumption of SAWs penetration approximately equals one wavelength. The result shows that our method has great potential to be applied in real clinical diagnosis of skin diseases as the SAWs penetration depth covered the dermis layer of skin where the pathological changes normally exist in.

References

Chunhui Li, S.L., Wenbin Xu, Zhihong Huang, *Skin Thermal Effect by FE Simulation and Experiment of Laser Ultrasonics.* Applied mechanics and materials, 2010. 24-25: p. 281-286.

Delalleau, A., et al., *Characterization of the mechanical properties of skin by inverse analysis combined with the indentation test.* Journal of Biomechanics, 2006. 39(9): p. 1603-1610.

Li, C., et al., *Finite element simulation of laser generated surface waves in layered skin model: effect of laser beam characteristics*. Vol. 7898. 2011: SPIE. 78980W.

Li, C., Z. Huang, and R.K. Wang, *Elastic properties of soft tissue-mimicking phantoms assessed by combined use of laser ultrasonics and low coherence interferometry.* Opt. Express, 2011. 19(11): p. 10153-10163.

Mariappan, Y.K., et al., *MR elastography of human lung parenchyma: Technical development, theoretical modeling and in vivo validation.* Journal of Magnetic Resonance Imaging, 2011. 33(6): p. 1351-1361.

Nightingale, K., S. McAleavey, and G. Trahey, *Shear-wave generation using acoustic radiation force: in vivo and ex vivo results.* Ultrasound in Medicine & Biology, 2003. 29(12): p. 1715-1723.

Pailler-Mattei, C., S. Bec, and H. Zahouani, *In vivo measurements of the elastic mechanical properties of human skin by indentation tests.* Medical Engineering & Physics, 2008. 30(5): p. 599-606.

Palmeri, M.L. and K.R. Nightingale, *Acoustic radiation force-based elasticity imaging methods.* Interface Focus, 2011. 1(4): p. 553-564.

Rivaz, H., et al., *Real-Time Regularized Ultrasound Elastography.* Medical Imaging, IEEE Transactions on, 2011. 30(4): p. 928-945.

Uff, C.E., et al. *Real-time ultrasound elastography in neurosurgery*. in *Ultrasonics Symposium (IUS), 2009 IEEE International*. 2009.

Wang, H. and et al., *A three-dimensional quality-guided phase unwrapping method for MR elastography.* Physics in Medicine and Biology, 2011. 56(13): p. 3935.

Zhu, Q.-L., et al., *Real-Time Ultrasound Elastography: Its Potential Role in Assessment of Breast Lesions.* Ultrasound in Medicine & Biology, 2008. 34(8): p. 1232-1238.